Third-order Nonlinear Optical Properties and Crystal Structures of *N*-(2-Nitrobenzalidene)-2,4-dimethylaniline and *N*-(3-Nitrobenzalidene)-2,4-dimethylaniline

Aslı Karakaş[a], Hüseyin Ünver[b], and Ayhan Elmalı[c]

[a] Department of Physics, Faculty of Arts and Sciences, Selçuk University, TR-42049 Campus, Konya, Turkey
[b] Department of Physics, Faculty of Sciences, Ankara University, Tandoğan, TR-06100 Ankara, Turkey
[c] Department of Engineering Physics, Faculty of Engineering, Ankara University, Tandoğan, TR-06100 Ankara, Turkey

Reprint requests to Dr. Hüseyin Ünver. Fax: +903122232395. E-mail: unver@science.ankara.edu.tr

Z. Naturforsch. **2007**, *62b,* 1437 – 1442; received May 30, 2007

N-(2-nitrobenzalidene)-2,4-dimethylaniline (**1**) and *N*-(3-nitrobenzalidene)-2,4-dimethylaniline (**2**) have been synthesized and characterized by X-ray diffraction analysis. Linear optical characteristics have been evaluated theoretically using the configuration interaction (CI) method. The maximum one-photon absorption (OPA) wavelengths of the studied compounds are shorter than 450 nm, giving rise to good optical transparency in the visible and near IR regions. To provide an insight into the third-order nonlinear optical (NLO) behavior of the title molecules, both dispersion-free (static) and frequency-dependent (dynamic) linear polarizabilities (α) and second hyperpolarizabilities (γ) at λ = 825 – 1125 nm and 1050 – 1600 nm wavelength ranges have been computed using the time-dependent Hartree-Fock (TDHF) method. The *ab initio* computational results on (hyper)polarizabilities reveal that both compounds exhibit second hyperpolarizabilities with non-zero values, implying microscopic third-order NLO behavior.

Key words: Third-order Optical Nonlinearity, One-photon Absorption, First Hyperpolarizability, Second Hyperpolarizability, Configuration Interaction

Introduction

In recent years, designing and synthesizing molecular materials with larger (hyper)polarizabilities are hot research topics [1 – 3], which relate to several fields, such as physics, medicine and chemistry. Along with linear and quadratic effects there has been growing interest in third-order optical nonlinearity. Due to potential applications in various photonic technologies, the nonlinear optical (NLO) properties of organic molecular materials have been the object of intense research [4]. Devices for applications in optical communications, optical processors, optical switches, wavelength filters and modulators have been created using the NLO response properties of organic systems. Therefore, organic molecules have been intensively studied with respect to their potential applications as NLO media [1, 5]. During the investigations of organic molecules for NLO, quantum chemical calculations have made an important contribution to the understanding of the (hyper)polarizabilities underlying the molecular third-order NLO processes and the establishment of structure-property relationships.

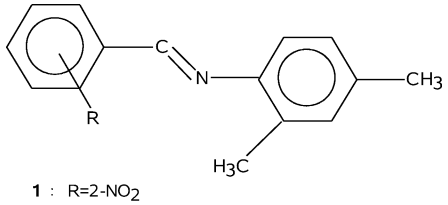

1 : R=2-NO_2
2 : R=3-NO_2

Fig. 1. Chemical structure of compounds **1** and **2**.

Among NLO molecules, the Schiff bases have gained special interest for many investigators because of their relatively large molecular hyperpolarizabilities due to delocalization of the π electrons [5, 6]. In general, Schiff base ligands may bear a variety of substituents with different electron-donating or electron-

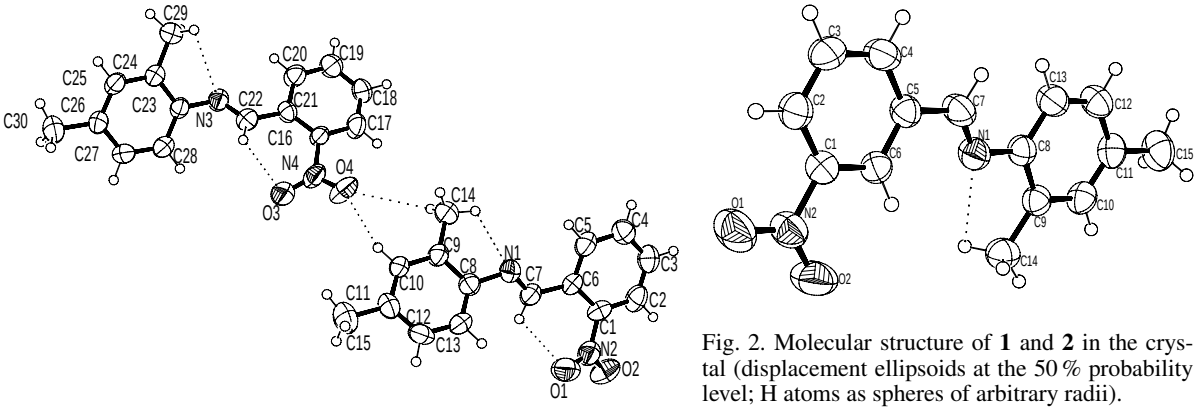

Fig. 2. Molecular structure of **1** and **2** in the crystal (displacement ellipsoids at the 50 % probability level; H atoms as spheres of arbitrary radii).

Table 1. Crystal and structure refinement data for **1** and **2**.

	1	**2**
Formula	$C_{15}H_{14}N_2O_2$	$C_{15}H_{14}N_2O_2$
M_r	254.28	254.28
Cryst. size, mm^3	$0.04 \times 0.24 \times 0.50$	$0.24 \times 0.24 \times 0.50$
Crystal system	triclinic	monoclinic
Space group	$P\bar{1}$	$C2/c$
a, Å	15.701(2)	15.701(2)
b, Å	5.909(1)	5.909(1)
c, Å	28.300(4)	28.300(4)
α, deg	94.06(1)	90
β, deg	94.48(1)	94.74(1)
γ, deg	103.32(1)	90
V, Å^3	1298.5(3)	2616.6(7)
Z	4	8
D_{calcd}, g cm^{-3}	1.30	1.29
μ(MoK_α), cm^{-1}	0.009	0.009
F(000), e	536	1072
hkl range	$\pm 9, \pm 10, +26$	$\pm 19, 0-7, +35$
$((\sin\theta)/\lambda)_{max}$, Å^{-1}	0.63	0.62
Refl. measured	5204	2673
Refl. unique	5182	2665
R_{int}	0.0312	0.0271
Param. refined	343	172
R_1/wR_2 [$I \geq 2\sigma(I)$]	0.065/0.122	0.058/0.124
Goodness-of-fit (F^2)	1.247	1.017
$\Delta\rho_{max/min}$, e Å^{-3}	0.20/−0.30	0.15/−0.20

withdrawing groups. Therefore, the effect of electron donor/acceptor substituents on the second hyperpolarizabilities of Schiff base molecules has received much attention in recent years. The aim of our present study is twofold: to characterize the newly synthesized Schiff bases shown in Fig. 1 having electron-donor methyl groups in *ortho* and *para* positions and also acceptor nitro groups in *ortho* and *meta* positions of **1** and **2**, respectively, with spectroscopic (UV/vis) and crystallographic (X-ray diffraction) techniques, and to investigate the third-order NLO behavior utilizing an *ab initio* time-dependent Hartree-Fock (TDHF) procedure on dispersion-free and frequency-dependent linear polarizabilities and second hyperpolarizabilities.

Table 2. Selected bond length (Å), angles (deg), and dihedral angles (deg) for **1** and **2** with estimated standard deviations in parentheses.

	1	**2**
Distances		
C1–C2	1.365(2)	1.373(2)
C1–N2	1.457(8)	1.464(1)
C9–C14	1.493(2)	1.496(2)
N2–O2	1.208(4)	1.215(1)
N2–O1	1.212(1)	1.229(1)
C8–N1	1.421(6)	1.419(1)
Angles		
C2–C1–C6	122.0(6)	122.7(1)
C4–C3–C2	118.8(0)	120.4(1)
O2–N2–C1	117.4(9)	118.7(1)
C7–N1–C8	116.6(7)	121.9(1)
Dihedral angles		
O1–N2–C1–C2	152.1(1)	2.2(2)
C14–C9–C8–N1	5.2(1)	−176.4(1)
C13–C8–N1–C7	48.4(1)	−4.8(2)
C1–C2–C3–C4	−0.41(1)	−0.2(2)

Experimental Section

*Preparation of compounds **1** and **2***

Compound **1** was prepared by condensation of 2-nitrobenzaldehyde (0.01 mol) and 2,4-dimethylaniline (0.01 mol) in 150 mL of ethanol. The reaction mixture was stirred for 4 h, and then placed in a freezer for 12 h. The precipitate was collected by filtration, and then washed with cold ethanol. It was crystallized from chloroform/*n*-heptane as yellow crystals. – M. p. 112 °C, 2.41 g (95 %) yield. – ^{1}H NMR (DMSO): δ = 9.60 (s, 1H, Ar–C*H*=N–Ar), 8.98 – 6.71 (m, 7H, Ar-*H*), 2.03 (s, 3H, Ar-C*H*$_3$), 2.01 (s, 3H, Ar-C*H*$_3$). – $C_{15}H_{14}N_2O_2$ (254.28): calcd. C 70.85, H 5.55; found C 70.56, H 5.53. Compound **2** was synthesized with the same procedure. – M. p. 128 °C, 2.36 g (93 %) yield. – ^{1}H NMR (DMSO):

δ = 9.47 (s, 1H, Ar–C*H*=N–Ar), 8.51 – 6.57 (m, 7H, Ar-*H*), 2.02 (s, 3H, Ar-CH_3), 2.00 (s, 3H, Ar-CH_3). – $C_{15}H_{14}N_2O_2$ (254.28): calcd. C 70.85, H 5.55; found C 70.76, H 5.51.

X-Ray structure determination

The data collection for both compounds was performed on an Enraf-Nonius diffractometer employing graphite-monochromatized MoK_α radiation (λ = 0.71073 Å). Data reduction and corrections for absorption and crystal decomposition of compounds **1** and **2** was carried out using the Nonius Diffractometer Control Software [7]. The structures were solved with SHELXS-97 [8] and refined with SHELXL-97 [9]. The positions of the H atoms bonded to C atoms were calculated, and included in the structure factor calculation using a riding model. The details of X-ray data collection, structure solution and structure refinements are given in Table 1. Bond lengths and angles are listed in Table 2. The molecular structures with the atom-numbering scheme are shown in Fig. 2 [10].

CCDC648357 and 648358 contain the supplementary crystallographic data for this paper. These data can be obtained free of charge from The Cambridge Crystallographic Data Centre *via* www.ccdc.cam.ac.uk/data_request/cif.

Theoretical calculations

The theoretical computations involve the determination of dispersion-free and frequency-dependent linear polarizability and second hyperpolarizability tensor components of the title compounds using the following methods:

Before the calculation of static and dynamic (hyper)polarizabilities for the investigated molecules, the geometries were optimized on the *ab initio* restricted closed-shell Hartree-Fock level. The optimized structures were used to compute the linear polarizabilities and third-order hyperpolarizabilities at ω frequencies with a 6-311+G(*d*, *p*) basis set. There are many well-established and tested computational codes to compute accurately the NLO properties of rather large molecular systems. Some of them are important as valuable theoretical tools used for the computation of (hyper)polarizabilities. The *ab initio* TDHF method is the most useful one among the computational procedures [4]. Calculations of $\alpha(0;0)$ and $\gamma(0;0,0,0)$ at $\omega = 0$, and $\alpha(-\omega;\omega)$ and $\gamma(-3\omega;\omega,\omega,\omega)$ at ω = 0.05512, 0.04050, 0.04336, 0.02848 atomic units (a. u.) (*i. e.* at λ = 825, 1125, 1050, 1600 nm wavelengths), often used laser frequencies in third-harmonic generation (THG) measurements, were carried out using the TDHF method implemented in the GAMESS program [11]. In the γ definitions mentioned above, the first one describes the static third-order hyperpolarizabilities, and the second represents the hyperpolarizability for frequency tripling, called the THG process.

The average linear polarizability $\langle\alpha\rangle$ and third-order hyperpolarizability $\langle\gamma\rangle$ values were calculated using the following expressions [12]:

$$\langle\alpha\rangle = \left(\alpha_{xx} + \alpha_{yy} + \alpha_{zz}\right)/3 \quad (1)$$

$$\langle\gamma\rangle = \frac{1}{5}\left[\gamma_{xxxx} + \gamma_{yyyy} + \gamma_{zzzz} + 2\left(\gamma_{xxyy} + \gamma_{xxzz} + \gamma_{yyzz}\right)\right] \quad (2)$$

Since α and γ values of the GAMESS output are reported in a. u., the calculated α and γ values were converted into the electrostatic units (esu) (1 a. u. $\alpha = 0.1482 \times 10^{-24}$ esu, 1 a. u. $\gamma = 5.0367 \times 10^{-40}$ esu). To calculate all the (hyper)polarizabilities, the origin of the Cartesian coordinate system *(x, y, z)* = 0, 0, 0 was chosen at the center of mass of the compounds **1** and **2**.

Besides, the $\pi \rightarrow \pi^*$ transition wavelengths (λ_{max}) of the lowest-lying electronic transition and the oscillator strengths (*f*) of these transitions for the investigated molecules were studied theoretically by electron excitation configuration interaction using the CIS/6-31G method in GAUSSIAN98W [13].

Results and Discussion

Description of the crystal structure

Schiff base compounds have been under investigation during the last years because of their potential applicability in optical communications and many of them were shown to have NLO behavior [14 – 16]. The title molecules **1** and **2** are not planar. For **1**, the two Schiff base moieties (C1–C7, O1, O2, N1) (planar with a maximum deviation of 0.080(1) Å for the O2 atom) and (N1, C8–C15) (planar with a maximum deviation of 0.076(1) Å for the N1 atom) are inclined at an angle of 7.76(1)°. Compound **2** has two independent molecules in the asymmetric unit. The two phenyl rings connected by the C=N imino moiety are inclined at angles of 31.6(1)° and 31.2(1)°, respectively.

The crystal structure of both **1** and **2** is stabilized by weak intramolecular and intermolecular hydrogen bonding [17 – 19]. Intramolecular hydrogen bonds occur between C7–H7A···O1 (2.723(2) Å), C14–H14A···N1 (2.798(2) Å), C22–H22A···O3 (2.737(2) Å), C29–H29A···N3 (2.754(2) Å) atoms in **1** and between C14–H14A···N1 (2.826(2) Å) in **2** (Fig. 2). The sum of the van der Waals radii of the O and N atoms (3.07 Å) is significantly larger than the intramolecular O···N hydrogen bond length [20]. There is also intermolecular hydrogen bonding between C14···O4 (3.582(2) Å) and C10···O4 (3.605(2) Å) in **1** and between C13···O2 (3.511(2) Å), (symmetry code:

Table 3. Calculated maximum UV/vis absorption wavelengths (λ_{max}, nm) and oscillator strengths (f) of compounds **1** and **2**.

	1	**2**		**1**	**2**
λ_{max}	416.31	419.40	f	2.1113	2.0010
	386.66	390.05		1.9877	1.6450
	259.50	278.24		1.5633	1.6020
	243.60	251.34		1.0008	1.1260

Table 4. Some selected components of the static $\alpha(0;0)$ and $\langle\alpha\rangle(0;0)$ [$\times 10^{-24}$ esu] values of compounds **1** and **2**.

	α_{xx}	α_{yy}	α_{zz}	$\langle\alpha\rangle$
1	33.56	17.81	4.05	18.47
2	34.64	17.17	4.02	18.61

$0.5+x$, $0.5+y$, z) atoms of neighboring molecules in **2** (Fig. 2).

Computational results and discussion

Quantum chemistry calculations have shown to be useful in the description of the relationship among the electronic structures of the systems and their NLO response [21]. NLO techniques are among the most structure sensitive methods to study molecular structures and assemblies [22]. The determination and analysis of the NLO properties of molecular systems with theoretical methods have greatly progressed during the past years. Actually, to accurately compute NLO properties of rather large molecular systems, there are well-tested computational codes.

It can be very helpful in the investigation of NLO materials to check, apart from NLO responses, also the spectroscopic absorbance in the appropriate wavelength. Thus, the wavelengths obtained by UV/vis spectral analysis can be helpful in planning the synthesis of promising NLO materials [23]. Since it is necessary to know the transparency region, electronic absorption spectral studies of compounds designed to possess NLO properties are important. In this paper, the vertical transition energies and oscillator strengths from the ground to the excited states have been computed, giving OPA, *i. e.*, the UV/vis spectrum. The calculated wavelengths (λ_{max}) and oscillator strengths (f) for the maximum OPA of the investigated molecules are shown in Table 3. Molecules **1** and **2** have four OPA peaks in their spectrum. As can be seen in Table 3, the optical spectra exhibit four relatively intense bands involving $\pi \rightarrow \pi^*$ transitions centered between 244 and 416 nm for compound **1** and between 252 and 419 nm for compound **2**. The values of all absorption maxima for both molecules are located in the UV region with wavelengths shorter than 450 nm, implying a good optical transparency in the visible region.

Table 5. Selected components of the frequency-dependent $\alpha(-\omega;\omega)$ and $\langle\alpha\rangle(-\omega;\omega)$ ($\times 10^{-24}$ esu) values at ω (in a. u.) laser frequencies for **1** and **2**.

		— ω —			
		0.05512	0.04050	0.04336	0.02848
α_{xx}	**1**	32.48	31.91	32.01	31.54
	2	33.45	32.97	33.04	32.74
α_{yy}	**1**	18.09	17.96	17.98	17.88
	2	17.43	17.30	17.33	17.23
α_{zz}	**1**	4.05	4.04	4.04	4.03
	2	4.00	3.99	3.99	3.98
$\langle\alpha\rangle$	**1**	18.21	17.97	18.01	17.82
	2	18.29	18.09	18.12	17.98

Table 6. All static $\gamma(0;0,0,0)$ components and $\langle\gamma\rangle(0;0,0,0)$ ($\times 10^{-37}$ esu) values for **1** and **2**.

	γ_{xxxx}	γ_{yyyy}	γ_{zzzz}	γ_{xxyy}	γ_{xxzz}	γ_{yyzz}	$\langle\gamma\rangle$
1	724.00	28.79	0.14	18.41	9.15	1.12	162.06
2	804.79	13.55	0.36	30.46	10.70	1.21	180.69

One could determine the hyperpolarizability tensors of molecules using a suitable computational approach. These tensors describe the response of molecules to an external electric field. At the molecular level, the NLO properties are determined by their dynamic hyperpolarizabilities. TDHF is a procedure generally used to find out approximate values and can help understanding both static and dynamic hyperpolarizabilities of organic molecules. We present here a comprehensive *ab initio* study of the NLO properties of the title molecules using the TDHF method. In this study, in addition to the static linear polarizabilities $\alpha(0;0)$ and second hyperpolarizabilities $\gamma(0;0,0,0)$, the following processess for dynamic (hyper)polarizabilities have been considered: frequency-dependent linear polarizabilities $\alpha(-\omega;\omega)$, THG $\gamma(-3\omega;\omega,\omega,\omega)$. Some significant calculated magnitudes of the static and frequency-dependent linear polarizabilities and second hyperpolarizabilities are shown in Tables 4 and 7, respectively.

Virtually high-order NLO effects in organic molecules originate from a strong intramolecular donor-acceptor interaction. The dipolar aromatic molecules possessing an electron donor group and an electron acceptor group contribute to large optical nonlinearity arising from the intramolecular charge transfer between the two groups of opposite nature. π-Conjugated molecules with a donor and an acceptor will not

Table 7. Selected components of the frequency-dependent $\gamma(-3\omega;\omega,\omega,\omega)$ and $\langle\gamma\rangle(-3\omega;\omega,\omega,\omega)$ ($\times 10^{-37}$ esu) values at ω (in a. u.) laser frequencies calculated with THG process for **1** and **2**.

		— ω —			
		0.05512	0.04050	0.04336	0.02848
γ_{xxxx}	**1**	4304.85	1373.24	1526.92	1191.17
	2	2960.11	1483.26	1619.60	1249.30
γ_{yyyy}	**1**	124.18	46.30	51.09	35.23
	2	34.51	19.89	21.41	16.51
γ_{zzzz}	**1**	−0.10	−0.22	−0.21	−0.26
	2	−0.18	−0.25	−0.24	−0.27
γ_{xxyy}	**1**	334.88	47.36	58.26	24.78
	2	53.32	39.63	42.02	33.62
γ_{xxzz}	**1**	5.42	2.74	2.79	4.19
	2	6.00	4.81	4.78	6.80
γ_{yyzz}	**1**	3.19	1.75	1.87	1.47
	2	1.71	1.50	1.59	1.29
$\langle\gamma\rangle$	**1**	1010.52	306.43	343.00	257.85
	2	658.22	325.09	355.84	270.89

display second-order NLO activity if they possess a center of symmetry. However, such centrosymmetric molecules might have third-order optical nonlinearity like the compounds studied here. More NLO chromophores can be envisaged using multiple donor and acceptor groups linked to different units of π conjugations. Although there are a few exceptions, a group may be an electron acceptor in one condition and an electron donor in another, depending on the situation. These acceptor-donor groups are generally attached to conjugated systems to generate NLO materials with large molecular hyperpolarizability in order to tailor their transparency. For the design of new organic materials such as Schiff bases one has to investigate the influence of donor-acceptor substituent positions upon the (hyper)polarizability values of these compounds; for instance at the *meta* position, the NLO behavior reacts most strongly on various substituents. Compounds **1** and **2** contain the same donor (-CH_3) in *ortho* and *para* positions at one end and an acceptor substituent (-NO_2) at the other differing only in the position at the aromatic ring. It can be seen from Tables 4 and 5 that static and dynamic polarizabilities of both compounds are not much affected by changing the substituent positions. We have found rather similar polarizabilities for compounds **1** and **2**. However, with a great possibility, the nitro group at the *meta* position enhances the static and dynamic third-order optical nonlinearity. Thus, $\langle\gamma\rangle$ values of compound **2** have been calculated to be larger than for compound **1** (see Tables 6 and 7). Compounds **1** and **2** may thus have microscopic third-order NLO behavior with non-zero (hyper)polarizabilities. It is also important to stress that, in the above α and γ calculations, we did not take into account the effect of the field on the nuclear positions, *i. e*. we evaluated only the electronic components of $\langle\alpha\rangle$ and $\langle\gamma\rangle$.

Conclusion

The title molecules have been synthesized, and their structures have been determined by X-ray diffraction. We have presented results of computational studies showing how the title compounds can possess third-order optical nonlinearity. To test the microscopic third-order NLO behavior computation of the OPA wavelengths, linear and second (hyper)polarizabilites of the studied compounds may be considered rather adequate. According to the results of the calculation on the linear optical behavior, the electronic transition wavelengths are estimated to be shorter than 450 nm, implying good optical transparency in the visible and near-IR region (450 – 900 nm). The *ab initio* calculated non-zero (hyper)polarizability values imply that the synthesized Schiff bases might have microscopic third-order NLO behavior.

Acknowledgement

This work was supported by the Turkish State of Planning Organization (DPT), TUBİTAK and Selçuk University under grant numbers 2003-K-12019010-7, 105T132, 2003/030, respectively.

[1] A. Elmali, A. Karakaş, H. Ünver, *Chem. Phys*. **2005**, *309*, 251.
[2] A. Karakaş, A. Elmali, H. Ünver, H. Kara, Y. Yahsi, *Z. Naturforsch*. **2006**, *61b*, 968.
[3] A. Karakaş, H. Ünver, A. Elmali, *J. Mol. Struct. (Theochem)* **2006**, *774*, 67.
[4] D. R. Kanis, M. A. Ratner, T. J. Marks, *Chem. Rev*. **1994**, *94*, 195.
[5] H. Ünver, A. Karakaş, A. Elmali, *J. Mol. Struct*. **2004**, *702*, 49.
[6] A. Karakaş, A. Elmali, H. Ünver, I. Svoboda, *Spectrochim. Acta Part A* **2005**, *61*, 2979.
[7] Enraf-Nonius Diffractometer Control Software (release 5.1.), Enraf-Nonius, Delft (The Netherlands) **1993**.
[8] G. M. Sheldrick, SHELXS-97, Program for the Solution

of Crystal Structures, University of Göttingen, Göttingen (Germany) **1997**.

[9] G. M. Sheldrick, SHELXL-97, Program for the Refinement of Crystal Structures, University of Göttingen, Göttingen (Germany) **1997**.

[10] L. J. Farrugia, *J. Appl. Crystallogr*. **1997**, *30*, 565.

[11] Intel × 86 (win32, Linux, O. S/2, D. OS) version. PC GAMESS (version 6.2), build number 2068. This version of GAMESS is described in: M. W. Schmidt, K. K. Baldridge, J. A. Boatz, S. T. Elbert, M. S. Gordon, J. H. Jensen, S. Koseki, N. Matsunaga, K. A. Nguyen, S. J. Su, T. L. Windus, M. Dupuis, J. A. Montgomery, *J. Comput. Chem*. **1993**, *14*, 1347.

[12] M. P. Bogaard, B. J. Orr in *MTP International Review of Science*, Vol. 2 (Ed.: A. D. Buckingham), Butterworths, London, **1975**, p. 149.

[13] M. J. Frisch, G. W. Trucks, H. B. Schlegel, G. E. Scuseria, M. A. Robb, J. R. Cheeseman, V. G. Zakrzewski, J. A. Montgomery, Jr., R. E. Stratmann, J. C. Burant, S. Dapprich, J. M. Millam, A. D. Daniels, K. N. Kudin, M. C. Strain, O. Farkas, J. Tomasi, V. Barone, M. Cossi, R. Cammi, B. Mennucci, C. Pomelli, C. Adamo, S. Clifford, J. Ochterski, G. A. Petersson, P. Y. Ayala, Q. Cui, K. Morokuma, D. K. Malick, A. D. Rabuck, K. Raghavachari, J. B. Foresman, J. Cioslowski, J. V. Ortiz, A. G. Baboul, B. B. Stefanov, G. Liu, A. Liashenko, P. Piskorz, I. Komaromi, R. Gomperts, R. L. Martin, D. J. Fox, T. Keith, M. A. Al-Laham, C. Y. Peng, A. Nanayakkara, C. Gonzalez, M. Challacombe, P. M. W. Gill, B. Johnson, W. Chen, M. W. Wong, J. L. Andres, C. Gonzalez, M. Head-Gordon, E. S. Replogle, J. A. Pople, GAUSSIAN98 (revision A.7), Gaussian Inc., Pittsburgh, PA (USA) **1998**.

[14] M. Jalali-Heravi, A. A. Khandar, I. Sheikshoaie, *Spectrochim. Acta A* **1999**, *55*, 2537.

[15] J. F. Nicoud, R. J. Twieg in *Nonlinear Optical Properties of Organic Molecules and Crystals*, Vol. 1 (Eds.: D. S. Chemla, J. Zyss), Academic Press, New York, **1987**, ch. 2.3, p. 277.

[16] M. Jalali-Heravi, A. A. Khandar, I. Sheikshoaie, *Spectrochim. Acta A* **2000**, *56*, 1575.

[17] G. Y. Yeap, S. G. Teoh, S. B. Teo, S. C. Loh, H. K. Fun, *Polyhedron* **1996**, *15*, 3941.

[18] B. Peng, G. Liu, L. Liu, D. Jia, K. Yu, *J. Mol. Struct*. **2004**, *692*, 217.

[19] G. Y. Yeap, S. T. Ha, N. Ishizawa, K. Suda, P. L. Boey, W. A. K. Mahmood, *J. Mol. Struct*. **2003**, *658*, 87.

[20] A. Bondi, *J. Phys. Chem*. **1964**, *68*, 441.

[21] J. L. Brédas, C. Adant, P. Tackx, A. Persoons, *Chem. Rev*. **1994**, *94*, 243.

[22] Y. R. Shen, *Proc. Natl. Acad. Sci. USA* **1996**, *93*, 112104.

[23] J. Kulakowska, S. Kucharski, *Eur. Polymer J*. **2000**, *36*, 1805.